Water vapor spectroscopy and thermodynamics constrain Earth's tropopause temperature

Brett A. McKim[1], **Nadir Jeevanjee**[2], **Geoffrey K. Vallis**[1], **Neil T. Lewis**[1]

[1]Department of Mathematics and Statistics, University of Exeter, Exeter, UK
[2]Geophysical Fluid Dynamics Laboratory, Princeton, NJ, USA

Key Points:

- We hypothesize that moisture and spectroscopy constrain the radiative tropopause temperature
- This prediction bears out quantitatively in both single column and general circulation model experiments
- Our derivation and results underpin the Fixed Tropopause Temperature (FiTT) hypothesis

Corresponding author: Brett A. McKim, brettmckim@gmail.com

Abstract

As Earth warms, the tropopause is expected to rise, but predictions of its temperature change are less certain. One theory ties tropopause temperature to outgoing longwave radiation (OLR), but this contradicts simulations that exhibit a Fixed Tropopause Temperature (FiTT) even as OLR increases. Another theory ties tropopause temperature to upper tropospheric moisture, but is not precise enough to make quantitative predictions. Here, we argue that tropopause temperature, defined by where radiative cooling becomes negligible, is set by water vapor's maximum spectroscopic absorption and Clausius-Clapeyron scaling. This "thermospectric constraint" makes quantitative predictions for tropopause temperature that are borne out in single column and general circulation model experiments where the spectroscopy is modified and the tropopause changes in response. This constraint underpins the FiTT hypothesis, shows how tropopause temperature can decouple from OLR, suggests a way to relate the temperatures of anvil clouds and the tropopause, and shows how spectroscopy manifests in Earth's general circulation.

Plain Language Summary

The tropopause separates the troposphere from the stratosphere, but theories disagree on the mechanisms that determine its temperature. We argue that the tropopause occurs where water vapor becomes so sparse that it can no longer emit radiation to space. The temperature this occurs at is set by how sensitive water vapor is to temperature and how effective it is in blocking and emitting radiation. Our theory leads to precise predictions of tropopause temperature and its change with surface warming. We verify our theory's mechanism by varying the effectiveness of water vapor absorption in climate models and find the tropopause temperature to change consistently with our theory's predictions. Our results suggest a role for wavelength-dependent radiation physics in constraining the large scale motions of Earth's atmosphere.

1 Introduction

The tropopause separates the overturning troposphere from a more idle stratosphere. Understanding the mechanisms setting tropopause temperature and height remains a fundamental and important unsolved problem in climate science (Phillips, 1956) — fundamental because it depends on how two branches of climate, dynamics and radiation, interact (Schneider, 2008; Vallis, 2017); important because the tropopause is a boundary condition in hurricane intensity (Emanuel, 2006; Emanuel et al., 2013), convectively available potential energy (Romps, 2016), CO_2 forcing (Jeevanjee et al., 2021), the water vapor feedback (Meraner et al., 2013; Koll et al., 2023; Feng et al., 2023), stratospheric water vapor (Mote et al., 1996), and ozone destruction (Match & Gerber, 2022).

The dynamically active troposphere is thought to extend upwards until the radiative equilibrium temperature profile of the stratosphere becomes stable to convection and eddies (Held, 1982; Thuburn & Craig, 2000), a condition known as the *radiative constraint* that defines a radiative tropopause as the lowest level at which the atmosphere attains radiative equilibrium. We focus on this radiative definition, but note that the tropopause can also be diagnosed with a lapse-rate criterion, and the two measures will often but not always be similar (Highwood & Hoskins, 1998), a point we return to later.

One way to understand the radiative tropopause temperature is in terms of top-of-atmosphere energy balance (Held, 1982; Thuburn & Craig, 2000; Vallis et al., 2015; Vallis, 2017). In this theory, *gray* radiative transfer (independent of wavenumber) and an optically thin stratosphere and upper troposphere are often assumed for conceptual simplicity. This lets tropopause temperature (T_{tp}) be regarded as a skin-like temperature (Pierrehumbert, 2010) dictated by the outgoing longwave radiation (OLR):

$$T_{\mathrm{tp}} = (\mathrm{OLR}/2\sigma)^{1/4} \quad \text{(OLR constraint)}, \tag{1}$$

where σ is the Stefan-Boltzmann constant. Note, though, that the source of the outgoing radiation still lies within the troposphere. This suggests a direct coupling between T_{tp} and OLR and makes no direct reference to the properties of Earth's greenhouse gasses. It predicts an unchanging tropopause temperature with CO_2-driven global warming, which is generally consistent with comprehensive climate models (Vallis et al., 2015; Hu & Vallis, 2019). It also suggests a sensitivity of T_{tp} to warming agents that increase OLR (such as an increase in insolation).

However, a fixed tropopause temperature (FiTT) has been shown in simulations of warming *without* fixed OLR (Seeley et al., 2019), which may be at odds with the OLR constraint. The expectation of a FiTT *independent* of the warming agent originates from an entirely different branch of research focused on the fixed temperature of anvil clouds in response to surface warming (Hartmann & Larson, 2002). In this theory, water vapor, the primary source of radiative cooling in the troposphere (Manabe & Strickler, 1964), is thought to control T_{tp}. Hartmann and Larson (2002); Harrop and Hartmann (2012) showed that tropical convection is tied to water vapor-driven radiative cooling. Moisture declines exponentially with temperature, until there is so little water vapor that it can no longer radiatively cool, thereby limiting the vertical extent of convection. These results were generalized and shown to apply to extratropical high clouds (Thompson et al., 2017, 2019), and Seeley et al. (2019) suggested that a similar hypothesis may be even more apt for the radiative tropopause. As evidence of this potential connection, Seidel and Yang (2022) showed that anvil clouds and the tropopause covary with surface warming.

If this is all true, then the temperature dependence of water vapor and its radiative cooling imposes a *moist thermodynamic constraint* on the tropopause. This is consistent with observations and models (Thompson et al., 2017, 2019) and helps explain the FiTT response to surface warming and its relation to Fixed Anvil Temperatures (FAT) (Hartmann & Larson, 2002; Seeley et al., 2019; Seidel & Yang, 2022). However, it makes no reference to OLR and it remains unclear what sets the temperature at which water vapor is unable to radiatively cool. The moist constraint cannot predict T_{tp}, and thus the FiTT hypothesis lacks a quantitative basis.

These limitations and contradictions may be resolved by noting that OLR *is* coupled to moist thermodynamics (Simpson, 1928; Nakajima et al., 1992; Koll & Cronin, 2018; Jeevanjee et al., 2021), and that spectral (wavenumber-dependent) theories of radiation can yield quantitative insights into this coupling (Feng et al., 2023; Koll et al., 2023). This approach led to a moist radiative theory for anvil cloud temperatures (Jeevanjee & Fueglistaler, 2020b) and we will follow suit to derive a more precise theory of the radiative tropopause temperature and of FiTT. Like Held (1982); Thuburn and Craig (2000), we study the radiative tropopause (henceforth "the tropopause"), but we will inspect the lapse rate tropopause and the role of dynamical constraints (Stone & Carlson, 1979; Held, 1982; Schneider, 2004, 2008; Schneider & O'Gorman, 2008; O'Gorman, 2011; Zurita-Gotor & Vallis, 2011; Vallis, 2017) later on. Stratospheric dynamics and ozone affect tropopause structure (Highwood & Hoskins, 1998; Thuburn & Craig, 2000, 2002; Fueglistaler et al., 2009; Birner, 2010; Lin et al., 2017; Dacie et al., 2019) and their inclusion is necessary to capture the full complexity of the tropopause response to climate change (Randel & Jensen, 2013). However, here we focus on more basic mechanisms that should be embedded in most climate models.

2 Formulating the thermospectric constraint

Qualitative overview

Understanding clear-sky radiative cooling is key to constraining the tropopause. The cooling profile is controlled by the wavenumber-dependence of water vapor spectroscopy (Jeevanjee & Fueglistaler, 2020b). At each temperature (or height), there are only a few

wavenumbers that cool (Jeevanjee & Fueglistaler, 2020a, 2020b), with colder temperatures (higher heights) cooling at wavenumbers with stronger spectroscopic absorption. We demonstrate this in a moist-adiabatic single column model at 300 K with line-by-line radiative transfer, PyRADS (Koll & Cronin, 2018). Plotting the spectrally-resolved cooling reveals that at any given height, most cooling is contained within a roughly 200 cm^{-1} width band whose contours mimic the V-shape of water vapor spectroscopy (Figure 1a,c).

Following this logic, water vapor's maximum spectroscopic absorption strength around 150 cm^{-1} (Figure 1a) suggests there is a minimum temperature (maximum height) to which water vapor can radiatively cool (Figure 1c). We argue that the *combination* of water vapor spectroscopy and Clausius-Clapeyron scaling constrains tropopause temperature. This *thermospectric constraint* refines the moist constraint with a more fundamental explanation for where and why water vapor's radiative cooling declines in the upper troposphere. It refines the OLR constraint into a spectral emission constraint that relates particular features of the radiative cooling profile to their corresponding emission temperatures.

Making the constraint quantitative

Small amounts of upper tropospheric water vapor can cool because of its strong radiative absorption in the rotational band (Figure 1a and Clough et al., 1992). Consider water vapor's optical depth:

$$\tau_{\mathrm{H_2O}}(\nu, z) = \int_z^\infty \kappa_{\mathrm{H_2O}}(\nu) \frac{p}{p_{\mathrm{ref}}} \rho_{\mathrm{H_2O}} dz', \tag{2}$$

where $\kappa_{\mathrm{H_2O}}(\nu)$ is the spectroscopic absorption strength of water vapor ($\mathrm{m}^2\ \mathrm{kg}^{-1}$) at wavenumber ν (cm^{-1}), p/p_{ref} accounts for pressure broadening at wavenumbers more than about 0.1 cm^{-1} away from line centers (Fu, 2006), p is the pressure, $p_{\mathrm{ref}} = 500$ hPa is a reference pressure, and $\rho_{\mathrm{H_2O}}$ is the density of water vapor. Infrared emission from water vapor peaks around $\tau_{\mathrm{H_2O}} \approx 1$ (Jeevanjee & Fueglistaler, 2020a; Jeevanjee, 2023), which implies an inverse relationship between $\kappa_{\mathrm{H_2O}}$ and the integral of $\rho_{\mathrm{H_2O}}$. $\kappa_{\mathrm{H_2O}}$ varies by many orders of magnitude across the infrared (Figure 1a), so many atmospheric levels emit to space (Figure 1c,d). However, a maximum in $\kappa_{\mathrm{H_2O}}$ implies a minimum $\rho_{\mathrm{H_2O}}$ and therefore a minimum temperature of the atmosphere that can effectively cool to space.

To formulate this statement quantitatively, we assume that all emission occurs at $\tau_{\mathrm{H_2O}} = 1$, which defines an emitting temperature T_{em} at wavenumber ν by the relation

$$\tau_{\mathrm{H_2O}}(\nu, T_{\mathrm{em}}) = 1. \tag{3}$$

It is more accurate to invert this equation numerically, but more informative to do so analytically, as shown in Jeevanjee and Fueglistaler (2020b); Jeevanjee (2023). We reproduce some of their steps for clarity.

The variable of integration in optical depth can be changed from height to temperature, and though water vapor spectroscopy varies due to pressure broadening, it varies much less than water vapor density does across the troposphere, so it can be pulled out of the integral. Optical depth is then proportional to water vapor path, which can be computed analytically (Koll & Cronin, 2018), resulting in a simplified expression:

$$\tau_{\mathrm{H_2O}}(\kappa_{\mathrm{H_2O}}, T) \approx \underbrace{\kappa_{\mathrm{H_2O}} \frac{p}{p_{\mathrm{ref}}}}_{\text{spectroscopy}} \underbrace{M_{\mathrm{v}} \mathrm{RH} \exp\left(-\frac{L}{R_{\mathrm{v}} T}\right)}_{\text{water vapor path}}, \tag{4}$$

where M_{v} is a characteristic column water vapor mass ($\mathrm{kg\ m}^{-2}$) and $M_{\mathrm{v}}\mathrm{RH}\exp(-L/R_{\mathrm{v}}T)$ is the column mass of water vapor above the isotherm with temperature T. Setting $\tau_{\mathrm{H_2O}} = 1$ and inverting it results in the emission temperatures as a function of absorption coefficients:

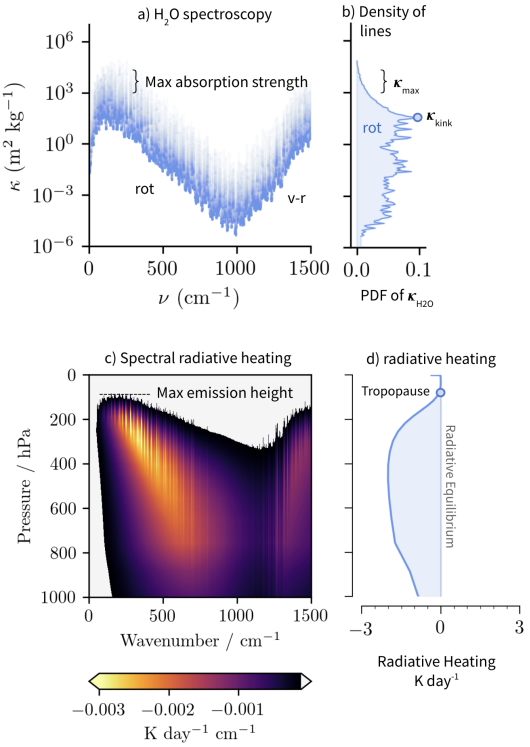

Figure 1. *The max absorption strength of water vapor spectroscopic absorption is hypothesized to constrain Earth's tropopause.* (a) Water vapor absorption strength as a function of wavenumber. (b) The rotational branch (150 to 1000 cm^{-1}) of absorption strength as a normalized histogram (plotted vertically), with units of $\ln \kappa_{H_2O}$. (c) Spectrally-resolved radiative cooling from a single column model with line-by-line radiative transfer, PyRADS. (d) Spectrally-integrated radiative cooling. We make a rough estimate of the maximum absorption coefficient as $\kappa_{max} \sim 10^3 - 10^4$ $m^2 kg^{-1}$, which we hypothesize relates to the tropopause. $\kappa_{kink} = 40$ m^2 kg^{-1} refers to where the density of lines begins to decline rapidly, which has been hypothesized to relate to anvil clouds (Jeevanjee & Fueglistaler, 2020b). Spectral data plotted at a resolution of 0.1 cm^{-1} using PyRADS (Koll & Cronin, 2018).

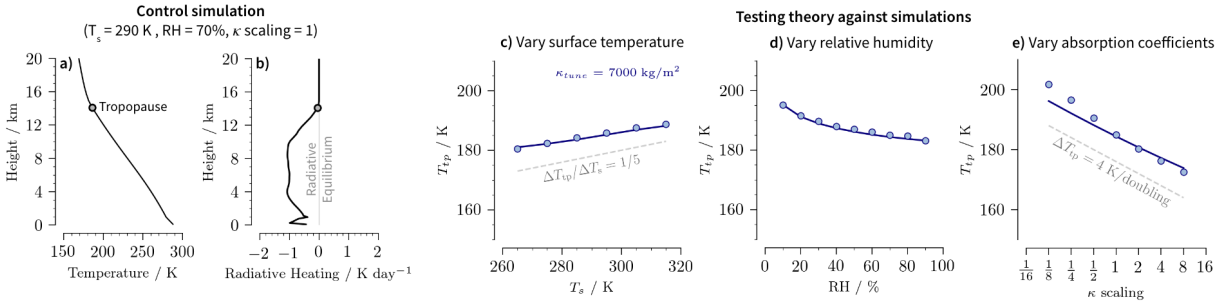

Figure 2. *The thermospectric constraint, Equation 5 and 6, can quantitatively capture the change in tropopause temperature (T_{tp}).* (a) Isca's single column model control simulation's temperature profile. (b) Control simulation's radiative cooling profile. (c) The surface temperature is varied and RH kept fixed at 0.7. Simulations (dots), theory (solid lines). (d) The relative humidity is varied and T_s fixed at 290 K. (e) The absorption coefficients of water vapor are scaled uniformly and T_s and RH fixed at 290 K and 0.7, respectively. Water vapor and CO_2 (280 ppmv) are the only greenhouse gases present in these simulations.

$$T_{\mathrm{em}}(\kappa_{\mathrm{H_2O}}) = \frac{T^*}{W\left(\frac{T^*}{T_{\mathrm{ref}}}(D \cdot \mathrm{RH} \cdot M_{\mathrm{v}} \cdot \kappa_{\mathrm{H_2O}})^{R_{\mathrm{d}}\Gamma/g}\right)}, \tag{5}$$

where T^* is a characteristic temperature for water vapor, W is the Lambert-W function, T_{ref} is a characteristic temperature of the troposphere, $D = 1.5$ is a scaling factor that accounts for the two stream approximation in radiative transfer theory, $R_{\mathrm{d}} = 287$ J kg^{-1} K^{-1} is the specific gas constant for dry air, $\Gamma = 7$ K km^{-1} is the globally-averaged lapse rate of the troposphere in the general circulation model used later on (Figure S1b), and g is the gravitational acceleration (see Table 1 in Methods for values and meanings of the variables and constants).

The thermospectric constraint posits that tropopause temperature T_{tp} is the emission temperature determined by a combination of Clausius-Clapeyron scaling (as embodied by RH and M_{v}) and the maximum absorption coefficient of water vapor, κ_{max}. That is,

$$T_{\mathrm{tp}} = T_{\mathrm{em}}(\kappa_{\mathrm{max}}). \quad \text{(Thermospectric constraint)} \tag{6}$$

The presence of thousands of absorption lines across the infrared (Figure 1a) makes it difficult to select an appropriate value of κ_{max}. It helps that the strength of spectrally integrated radiative cooling is roughly proportional to the density of absorption lines at a given strength (Figure 1b,d and Jeevanjee & Fueglistaler, 2020b). For values of $\kappa_{\mathrm{H_2O}} \in (10^{-4}, 10^{1})$ m^2 kg^{-1}, which correspond to tropospheric emission and a typical value of -2 K day^{-1} of radiative cooling (Jeevanjee & Fueglistaler, 2020b), the density of absorption lines in the rotational band (150 to 1000 cm^{-1}) has a characteristic value of $0.07 \ln \kappa_{\mathrm{H_2O}}$ (Figure 1b). The vibrational-rotational band (1000 to 1500 cm^{-1}) is not as important because its Planck emission is about 1/6 of the rotational band's emission (Jeevanjee & Fueglistaler, 2020b).

The proportionality between the density of lines and the strength of cooling provides a heuristic way to determine κ_{max}: look for where the density of lines drops between a tenth and a hundredth of its density for tropospheric emission, as this would roughly correspond to where cooling drops to between a tenth and a hundredth of its tropospheric value (thereby achieving radiative equilibrium) (Figure 1b,d). Other factors influence the strength of cooling, such as the change in optical depth with height and the strength of the Planck function at a given wavenumber and temperature, but (Jeevanjee & Fueglistaler, 2020b) showed that these cannot explain the declining strength of cooling in the upper troposphere.

We plot the density of absorption lines in the rotational band in Figure 1b. The density drops to between a tenth and a hundredth of its typical value at $\kappa_{\mathrm{H_2O}} \in (4 \cdot 10^3, 4 \cdot 10^4)$ m^2 kg^{-1}. Taking the geometric average of the upper and lower bounds, we arrive at our estimate of $\kappa_{\mathrm{max}} \approx 13000$ m^2 kg^{-1}. Plugging into Equation 6, our prediction for the tropopause temperature is $T_{\mathrm{tp}} \approx 180$ K.

3 Testing the thermospectric constraint

To test the thermospectric constraint (Equation 6), we run simulations using a clear-sky single column model (SCM) configuration of the Isca modeling framework (Vallis et al., 2018). The SCM is configured with the correlated-k radiative transfer code RRTM (Mlawer et al., 1997), and a simplified representation of moist convection (the simple Betts-Miller code of Frierson, 2007 and O'Gorman & Schneider, 2008). Configuring the SCM using Isca lets us compare to general circulation model (GCM) simulations with identical column-wise physics later in the paper. Further description of our model set-up can be found in the Supporting Information.

To begin, we consider an SCM control run with a prescribed surface temperature of $T_{\mathrm{s}} = 290$ K, relative humidity RH$= 0.7$, and CO_2 concentration of 280 ppmv. The diagnosed

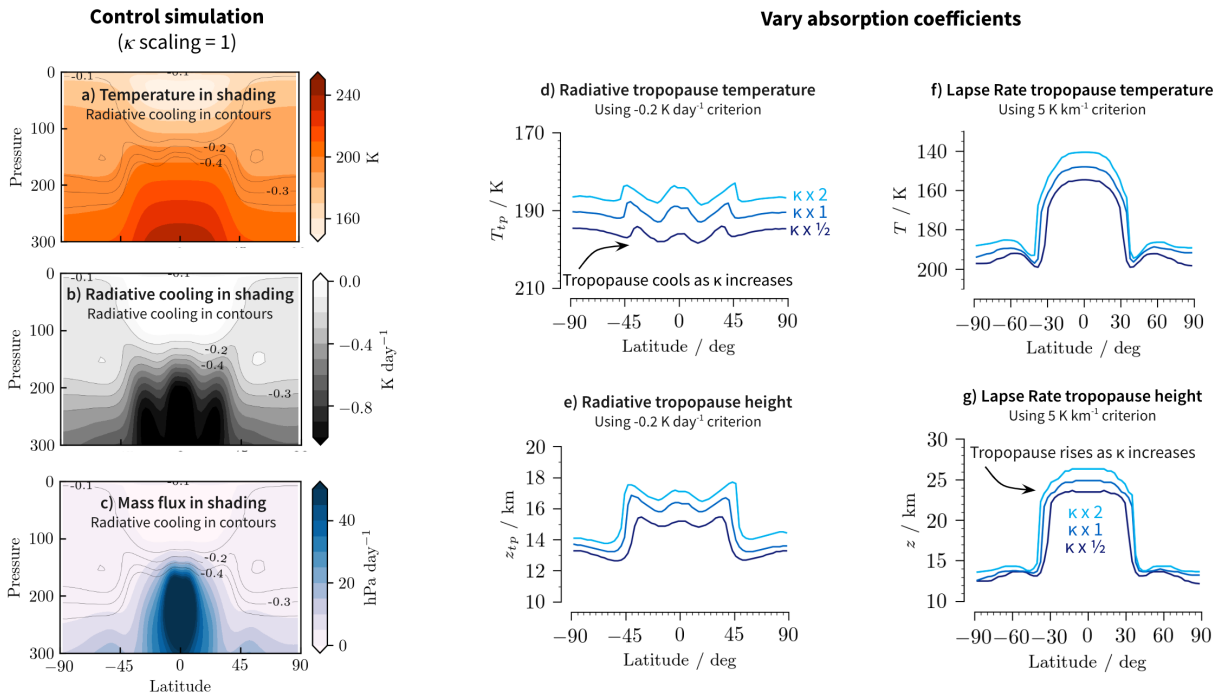

Figure 3. *Water vapor spectroscopy affects the radiative and lapse rate tropopauses.* (a) Zonal-mean temperature profile of the control Isca aquaplanet simulation. (b) Zonal-mean radiative cooling profile of the control. (c) Zonal-mean mass flux profile of the control. (d-g) Water vapor absorption coefficients are increased geometrically by [1/2, 1, 2] and the resulting changes in radiative- and lapse rate-tropopause temperature and height are recorded. The lack of ozone in these simulations accounts for the high (25 km) lapse rate tropopause.

tropopause temperature obtained in this simulation (the lowest level to which radiative equilibrium is achieved, which we identify as -0.05 K day^{-1} to avoid sensitivity issues related to the cooling profile's asymptotic approach to 0 K day^{-1}, see Figure 2a,b and Supporting Information), is 184 K, close to our prediction.

The maximum absorption coefficient of water vapour, $\kappa_{\max}$, can also be considered a free parameter to match the predicted tropopause temperature with the value diagnosed from a climate model. Tuning $\kappa_{\max}$ results in a value of 7000 m^2 kg^{-1}, which is within our identified range for $\kappa_{\max}$ based on the density of absorption lines. This tuned value is used henceforth and will not be retuned, except where explicitly scaled. Regarding this climate as our base state, we can test the thermospectric constraint by varying the prescribed surface temperature, column relative humidity, and absorption coefficients of water vapor in the SCM and see how well theory compares.

Surface temperature

As surface temperature increases, the thermospectric constraint (Equation 6) predicts a small but nonzero warming of the tropopause of about $\Delta T_{\mathrm{tp}}/\Delta T_{\mathrm{s}} = 1/5$ (Figure 2c, solid line). The slight warming is a second order effect from pressure broadening (Koll et al., 2023; Feng et al., 2023) which can be understood as follows. The tropopause temperature is fixed, to first order, which implies a rising tropopause as surface temperature increases. As pressure decreases, the effective water vapor absorption coefficients ($\kappa_{\mathrm{H_2O}} \cdot p/p_{\mathrm{ref}}$) also decreases, which implies a larger $\rho_{\mathrm{H_2O}}$ is needed to achieve $\tau_{\mathrm{H_2O}} = 1$, and thus a slightly warmer tropopause temperature. A simple calculation shows that the change in water vapor emission temperatures (including at the tropopause) should be about 1/4 to 1/5 of the warming at the surface (Equation B4 of Jeevanjee, 2023 and Equation 46 of Koll et al., 2023).

In an SCM experiment where surface temperature is increased (Figure 2c, dots), the tropopause warms almost exactly as predicted. The relatively fixed tropopause temperature (FiTT) has been noted before (Seeley et al., 2019) and explained qualitatively by Thompson et al. (2019) with the thermodynamic constraint. However, the thermospectric constraint provides a quantitative understanding of how T_{tp} should change with warming. The pressure broadening explanation differs from Hu and Vallis (2019), who explains the slight warming as a consequence of increased longwave radiation from outside the water vapor window.

Relative humidity

Variations in column relative humidity (RH) may influence T_{tp}. A larger RH implies a smaller saturation water vapor density $\rho^{\mathrm{sat}}_{\mathrm{H_2O}}$ to reach $\tau_{\mathrm{H_2O}} = 1$, and thus a cooler temperature. We vary RH in the SCM but keep surface temperature fixed and find the tropopause cools as RH increases (Figure 2d), in excellent agreement with predictions from inputting RH into the thermospectric constraint (Equation 5).

Water vapor absorption

Modifying the $\rho_{\mathrm{H_2O}}$ passed to the radiation code of a climate model alters the temperature of anvil clouds and the tropopause (Harrop & Hartmann, 2012; Thompson et al., 2019; Spaulding-Astudillo & Mitchell, 2023). The thermospectric constraint suggests that modifying $\kappa_{\mathrm{H_2O}}$ should have a similar effect. A geometrically larger $\kappa_{\max}$ implies a geometrically smaller minimum $\rho_{\mathrm{H_2O}}$ to achieve $\tau_{\mathrm{H_2O}} = 1$ and hence an arithmetically colder T_{tp} due to Clausius-Clapeyron scaling: $d \ln \rho_{\mathrm{H_2O}}/dT|_{T_{\mathrm{tp}}} = L/(R_{\mathrm{v}} T^2_{\mathrm{tp}}) = 16\%$ K^{-1} or roughly 4 K of cooling to halve $\rho_{\mathrm{H_2O}}$. These predictions are borne out quantitatively by the simulations, where T_{tp} cools arithmetically as $\kappa_{\max}$ is scaled geometrically over many octaves while T_{s} and RH are fixed, at a rate of roughly 4 K per doubling (Figure 2e). This is the most direct

test of the thermospectric constraint and it confirms spectroscopy's key role in constraining T_{tp}.

4 From spectroscopy to the general circulation

The previous tests were done in a single column model, but the tropopause is a feature of Earth's general circulation and will be influenced by other factors (Thuburn & Craig, 2000; Birner, 2010). We test whether modifying $\kappa_{\mathrm{H_2O}}$ influences T_{tp} and z_{tp} (tropopause height) in a general circulation model configured as an idealized aquaplanet with a standard fixed sea surface temperature distribution (Neale & Hoskins, 2000):

$$T_s(\phi) = \begin{cases} 300\big(1 - \sin^2(3\phi/2)\big)\ \mathrm{K}, & \text{for } -\pi/3 < \phi < \pi/3 \\ 273\ \mathrm{K}, & \text{otherwise,} \end{cases} \tag{7}$$

where ϕ is the latitude. The GCM is configured to use the same column-wise physics routines (e.g., RRTM radiative transfer, simplified Betts-Miller moist convection) as the SCM. See the Supporting Information for further details. When analysing the GCM, we diagnose the radiative tropopause with a -0.2 K day^{-1} threshold instead of the -0.05 K day^{-1} used for the SCM. The updated threshold more closely aligns with relevant dynamical features such the mass flux profile (Figure 3c) while still using a threshold value $\ll$ typical tropospheric cooling (Figure 3b).

Spectroscopic control of the tropopause

We vary $\kappa_{\mathrm{H_2O}}$ geometrically and find the tropopause cools and rises across all latitudes, again at $\approx 4-5$ K and $0.5-1$ km per doubling of $\kappa_{\mathrm{H_2O}}$ (Figure 3d,e). This cooling confirms the quantitative predictions of thermospectric constraint (Figure 2e) in a more comprehensive and Earth-like setting. The spectroscopic control on the radiative tropopause has implications for the general circulation because infrared cooling constrains the residual motion of the atmosphere, the amplitude of tropospheric wave breaking, and the depth of its diabatic mixing (Thompson et al., 2017, 2019).

T_{tp} varies by only 5 K across latitude in these simulations, consistent with FiTT and the idea of a fairly insensitive radiative tropopause temperature to surface temperature and the large-scale circulation. However, radiative tropopause *height* is not uniform due to its strong dependence on surface temperature and vertically averaged lapse rate (Γ), $z_{\mathrm{tp}} \approx (T_{\mathrm{tp}} - T_{\mathrm{s}})/\Gamma$. It has a top-hat meridional structure because T_{s} varies from equator to poles and because Γ varies as the dominant control on stratification changes from moist convection in the tropics to baroclinic eddies in the extratropics (Stone & Carlson, 1979; Held, 1982; Schneider, 2008; Vallis, 2017).

This dynamical control extends to the lapse-rate tropopause, diagnosed here as where the lapse rate exceeds -5 K km^{-1}. It has a much more pronounced top-hat structure in *both* its height and temperature (Figure 3f,g). FiTT does not apply to all definitions of the tropopause because each definition respects different physical constraints (Highwood & Hoskins, 1998; Fueglistaler et al., 2009; Birner, 2010; Hu & Vallis, 2019). The lapse rate tropopause, for instance, depends on the profile of stratification, which is primarily determined by dynamics (Schneider, 2008). Nevertheless, the lapse rate tropopause still cools and rises as $\kappa_{\mathrm{H_2O}}$ is increased (Figure 3f,g), particularly in the tropics, hinting at a broader role of spectroscopy in the interaction between upper tropospheric radiative cooling, dynamics, and stratification which future work could make more precise.

Other controls of the tropopause

Meridional variations in radiative tropopause temperature may be due to surface temperature, which varies between 300 K and 273 K from equator to poles and can change

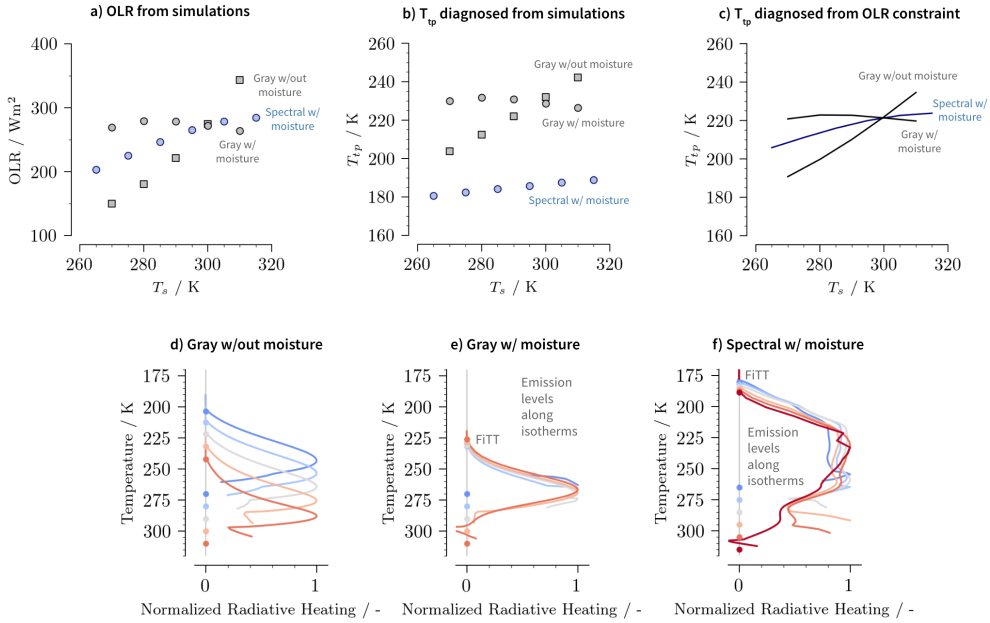

Figure 4. *Moisture is essential to capturing a fixed tropopause temperature and spectral radiative transfer decouples tropopause temperature from outgoing longwave radiation.* (a) Outgoing longwave radiation (OLR) of Isca single column model with various types of radiative transfer. (b) Tropopause temperature for the same simulations. (c) Predicted tropopause temperature from the OLR constraint (Equation 1). (d-f) The radiative cooling profile plotted in temperature coordinates for $T_s = 270, 280, 290, 300, 310$ K for each model setup. Each profile has been normalized by its maximum tropospheric value and is plotted starting at the lifting condensation level for clarity. See Supporting Information for details.

T_{tp} with pressure-broadening effects. It may also be due to tropospheric relative humidity, which varies from 20 to 70 % (Figure S1a). The SCM and Equation 5 shows varying column relative humidity by a similar amount changes T_{tp} by about 5 K (Figure 2d). The lapse rate (Figure S1b) could also change T_{tp}; changing Γ from 4 K km^{-1} to 7 K km^{-1} in Equation 5 changes T_{tp} by 3 K.

Column-wise physics and water vapor may not be the only source of variations in T_{tp}. Stratospheric dynamics may influence z_{tp} and T_{tp} by altering the location of zero radiative cooling (Thuburn & Craig, 2000; Birner, 2010; Hu & Vallis, 2019). CO_2-driven radiative cooling, which primarily emanates from the stratosphere (Jeevanjee & Fueglistaler, 2020b), may also drive changes in T_{tp}. Future work could address these questions and lead to a more comprehensive theory, but our goal here is to provide a first order picture of moist thermodynamics interact with spectroscopy to set T_{tp}.

5 Reconciling different constraints

Previous theories of tropopause temperature have either emphasized outgoing radiation (Held, 1982; Thuburn & Craig, 2000; Vallis et al., 2015) *or* moist thermodynamics and upper tropospheric radiative cooling (Hartmann & Larson, 2002; Thompson et al., 2017). Combining moisture with a spectral perspective of radiative cooling can make more precise predictions for T_{tp} and FiTT (Figure 2c). Now we combine the OLR constraint (Equation 1) with moisture to make better predictions of FiTT, and consider how adding bands to gray

radiative transfer theory morphs the OLR constraint into an upper tropospheric radiative emission constraint.

The OLR constraint was derived with gray radiative transfer uncoupled to moisture (Held, 1982; Thuburn & Craig, 2000; Vallis et al., 2015). This "dry" constraint predicts a FiTT with respect to CO_2-driven global warming because OLR remains fixed (Vallis et al., 2015). By this logic, a warming that changes OLR would change T_{tp}, which stands in contrast to simulations that exhibit a FiTT even as OLR increases (Seeley et al., 2019; Seidel & Yang, 2022). For both gray and spectral atmospheres, the amount of OLR increase for a prescribed surface warming depends on the presence of radiatively active moisture and its optical thickness (Simpson, 1928; Nakajima et al., 1992; Ingram, 2010; Koll & Cronin, 2018; Jeevanjee et al., 2021; Feng et al., 2023; Stevens & Kluft, 2023; Koll et al., 2023). Changes in T_{tp} may be similarly constrained.

We test the role of moisture and choice of radiative transfer in controlling OLR and T_{tp} by varying surface temperature in different configurations of Isca's SCM: a model with gray radiation uncoupled to moisture, similar to Frierson et al. (2006); with gray radiation coupled to moisture, similar to Byrne and O'Gorman (2013); and with spectral radiation coupled to moisture, as already described. In these experiments, OLR and T_{tp} change much more in the dry gray model than the moist gray and spectral models (Figure 4a,b).

In dry simulations, the greenhouse gas is assumed to be well mixed and so optical depth is a single valued function of pressure, $\tau = \tau(p)$. As T_{s} increases, isobars warm and radiative cooling at $\tau = 1$ emanates from a warmer layer of atmosphere that can emit more radiation to space (Figure 4d). In contrast, moisture constrains the optical depth to be a single valued function of temperature, $\tau = \tau(T)$ (in the absence of pressure broadening). As T_{s} increases, radiative cooling at $\tau = 1$ emanates from nearly the same temperature (Figure 4e,f and Figure S1a of Seeley et al., 2019) and thus OLR is constrained to increase less than in the dry case. (Radiative cooling can increase for other reasons, see, e.g., Jeevanjee & Romps, 2018, but less so if there is moisture.) Therefore, the OLR constraint, when combined with a notion of how moisture constrains changes in OLR, is more consistent with FiTT for a wider variety of warming scenarios such as in Seeley et al. (2019); Seidel and Yang (2022).

However, this explanation still does not address a motivating question of this study: How can T_{tp} decouple from OLR (compare Figure 4b,c)? The answer lies in the role of additional bands of radiative transfer. Hu and Vallis (2019) showed that adding a window band decouples the radiative equilibrium temperature of the planet, T_{re}, from total OLR and couples it instead to outgoing radiation from the optically thick band ($\mathrm{OLR}_{\mathrm{thick}}$):

$$T_{\mathrm{re}} = \left[\frac{\tau_{\mathrm{thick}} + 1}{2\sigma}\mathrm{OLR}_{\mathrm{thick}}\right]^{1/4}. \tag{8}$$

The window band becomes optically thin at the surface, so its emission does not contribute to radiative balance at the stratosphere (Hu & Vallis, 2019). If a third, even thicker band were introduced, then this logic implies that the thickest band's emission would determine the radiative balance at the stratosphere and constrain T_{re}, rather than the emission from the thinner bands. If we take the spectral limit of an infinite number of bands that vary by orders of magnitude in their optical depth, which is the case for Earth's atmosphere, then T_{re} would be determined primarily by the optically thickest band and constrained by its spectral emission. T_{re} (and hence T_{tp}) would be related to the brightness temperature of that spectral emission. This is essentially what we have calculated in the thermospectric constraint (Equations 5 and 6), though framed in a different way. The OLR constraint is only strictly true for a gray atmosphere, and the thermospectric constraint is the generalization of that idea to a spectral, moist atmosphere. Hence, T_{tp} can decouple from OLR, as seen in simulations of FiTT (Figure 4c and Seeley et al., 2019; Seidel & Yang, 2022).

6 Discussion

Summary

Spectral radiative transfer decouples Earth's radiative tropopause temperature from the total outgoing radiation and constrains it instead to where water vapor becomes optically thin across *all* wavenumbers and stops radiative cooling. This is set by water vapor's maximum spectroscopic absorption and Clausius-Clapeyron scaling. The thermospectric constraint implies a relatively fixed radiative tropopause temperature (FiTT) with warming because isopleths of water vapor path follows isotherms. However, pressure broadening modifies the strength of spectroscopic absorption as the tropopause rises with surface warming, causing it to warm slightly. FiTT also constrains the meridional distribution of the radiative tropopause, but not the lapse rate tropopause, which is more strongly controlled by dynamics than by radiation. The thermospectric constraint does not rule out a role for processes such as the Brewer-Dobson circulation (which is relatively weak in an aquaplanet, but can affect the tropopause height; Thuburn & Craig, 2000; Birner, 2010; Hu & Vallis, 2019) and ozone (which is not present in our simulations but can affect stratospheric temperature; Thuburn & Craig, 2000, 2002; Lin et al., 2017; Dacie et al., 2019), but it does suggest a previously unnoticed mechanism grounded in robust physics is important in controlling tropopause temperature.

Anvil clouds and the tropopause

The temperature of anvil clouds and the tropopause respond similarly to surface warming (Seidel & Yang, 2022), despite their ≈ 5 km difference in height (Seeley et al., 2019). The thermospectric constraint offers an explanation. Anvil clouds and the tropopause share a thermodynamic control by water vapor, which is why they respond similarly to warming, but they depend on distinct features of water vapor spectroscopy, so they occur at different temperatures. The radiative tropopause occurs where radiative cooling goes to zero, which is controlled by the maximum spectroscopic absorption ($\kappa_{\max} \approx 13000$ m^2 kg^{-1}): $T_{\mathrm{tp}} = T_{\mathrm{em}}(\kappa_{\max}) \approx 180$ K. Anvil clouds occur near the max vertical derivative of radiative cooling (Hartmann & Larson, 2002), which is controlled by the *sharp decline* in water vapor's emission line density at $\kappa_{\mathrm{kink}} = 40$ m^2 kg^{-1}: $T_{\mathrm{anvil}} = T_{\mathrm{em}}(\kappa_{\mathrm{kink}}) \approx 214$ K (Jeevanjee & Fueglistaler, 2020b). These thermodynamic and spectroscopic ingredients are embedded in most climate models, which could be why the relationship between anvil clouds and the tropopause are robust with respect to modeling configuration (Seidel & Yang, 2022).

A role for gray radiative transfer in studying climate?

Water vapor's thermodynamic and radiative properties have distinct but equally profound influences on Earth's climate (Held & Soden, 2006; Stevens & Bony, 2013), but are gray models of radiative transfer fit for understanding these influences? Gray climate models can capture the interplay of latent heat release and the general circulation (Frierson et al., 2006; Schneider et al., 2010; Vallis, 2020), some of the interaction between radiation and moisture necessary for water vapor feedbacks (Byrne & O'Gorman, 2013) and the runaway greenhouse effect (Nakajima et al., 1992), and can offer a qualitative understanding of Earth's greenhouse effect (Pierrehumbert, 2010).

However, many circulation responses to warming depend sensitively on the radiative response to warming (Kang et al., 2009; Voigt & Shaw, 2015; Ceppi & Hartmann, 2016; Tan et al., 2019), which stresses the need for more nuanced understanding of radiation. For the problems where a quantitative answer is desired, such as the forcing from CO_2 (Jeevanjee et al., 2021; He et al., 2023), water vapor feedback (Koll et al., 2023; Feng et al., 2023), and equilibrium climate sensitivity (Jeevanjee, 2023; Stevens & Kluft, 2023); or for the problems involving vertical gradients in radiative cooling, such as the temperature of anvil clouds (Hartmann & Larson, 2002; Jeevanjee & Fueglistaler, 2020b), radiation's wavenum-

ber dependence matters. Spectral theories promise to be the more powerful approach to identifying, studying, and potentially resolving them.

7 Open Research

All scripts used to support the creation and analysis of climate modeling data will be made available in a Github repository upon acceptance.

8 Author contributions

B.A.M, G.K.V., and N.J. designed research; B.A.M. performed research. B.A.M, G.K.V., and N.J. interpreted results and analyzed data; B.A.M wrote the first draft of the paper; N.L. created the single column model implementation in Isca.

Acknowledgments
This work was funded by CEMPS at the University of Exeter. GKV also acknowledges support from NERC under the CIRCULATES grant `NE/T006285/1`. We declare no known conflicts of interest.

References

Birner, T. (2010). Residual circulation and tropopause structure. *Journal of the Atmospheric Sciences*, *67*(8), 2582 - 2600. doi: https://doi.org/10.1175/2010JAS3287.1

Byrne, M. P., & O'Gorman, P. A. (2013). Land–ocean warming contrast over a wide range of climates: Convective quasi-equilibrium theory and idealized simulations. *Journal of Climate*, *26*(12), 4000 - 4016. doi: https://doi.org/10.1175/JCLI-D-12-00262.1

Ceppi, P., & Hartmann, D. L. (2016). Clouds and the atmospheric circulation response to warming. *Journal of Climate*, *29*(2), 783 - 799. doi: 10.1175/JCLI-D-15-0394.1

Clough, S. A., Iacono, M. J., & Moncet, J.-L. (1992). Line-by-line calculations of atmospheric fluxes and cooling rates: Application to water vapor. *Journal of Geophysical Research: Atmospheres*, *97*(D14), 15761-15785. doi: https://doi.org/10.1029/92JD01419

Dacie, S., Kluft, L., Schmidt, H., Stevens, B., Buehler, S. A., Nowack, P. J., ... Birner, T. (2019). A 1d rce study of factors affecting the tropical tropopause layer and surface climate. *Journal of Climate*, *32*(20), 6769 - 6782. doi: https://doi.org/10.1175/JCLI-D-18-0778.1

Emanuel, K. (2006, August). Hurricanes: Tempests in a greenhouse. *Physics Today*, *59*(8), 74–75. doi: 10.1063/1.2349743

Emanuel, K., Solomon, S., Folini, D., Davis, S., & Cagnazzo, C. (2013). Influence of tropical tropopause layer cooling on atlantic hurricane activity. *Journal of Climate*, *26*(7), 2288 - 2301. doi: https://doi.org/10.1175/JCLI-D-12-00242.1

Feng, J., Paynter, D., & Menzel, R. (2023). How a stable greenhouse effect on earth is maintained under global warming. *Journal of Geophysical Research: Atmospheres*, *128*(9), e2022JD038124. doi: https://doi.org/10.1029/2022JD038124

Frierson, D. M. W. (2007). The dynamics of idealized convection schemes and their effect on the zonally averaged tropical circulation. *Journal of the Atmospheric Sciences*, *64*(6), 1959 - 1976. doi: https://doi.org/10.1175/JAS3935.1

Frierson, D. M. W., Held, I. M., & Zurita-Gotor, P. (2006). A gray-radiation aquaplanet moist gcm. part i: Static stability and eddy scale. *Journal of the Atmospheric Sciences*, *63*(10), 2548 - 2566. doi: https://doi.org/10.1175/JAS3753.1

Fu, Q. (2006). 4 - radiative transfer. In J. M. Wallace & P. V. Hobbs (Eds.), *Atmospheric science (second edition)* (Second Edition ed., p. 113-152). San Diego: Academic Press. doi: https://doi.org/10.1016/B978-0-12-732951-2.50009-0

Fueglistaler, S., Dessler, A. E., Dunkerton, T. J., Folkins, I., Fu, Q., & Mote, P. W. (2009). Tropical tropopause layer. *Reviews of Geophysics*, *47*(1). doi: https://doi.org/10.1029/2008RG000267

Harrop, B. E., & Hartmann, D. L. (2012). Testing the role of radiation in determining tropical cloud-top temperature. *Journal of Climate*, *25*(17), 5731 - 5747. doi: https://doi.org/10.1175/JCLI-D-11-00445.1

Hartmann, D. L., & Larson, K. (2002). An important constraint on tropical cloud - climate feedback. *Geophysical Research Letters*, *29*(20), 12-1-12-4. doi: https://doi.org/10.1029/2002GL015835

He, H., Kramer, R. J., Soden, B. J., & Jeevanjee, N. (2023). State dependence of co2 forcing and its implications for climate sensitivity. *Science*, *382*(6674), 1051-1056. doi: 10.1126/science.abq6872

Held, I. M. (1982). On the height of the tropopause and the static stability of the troposphere. *Journal of Atmospheric Sciences*, *39*(2), 412 - 417. doi: https://doi.org/10.1175/1520-0469(1982)039⟨0412:OTHOTT⟩2.0.CO;2

Held, I. M., & Soden, B. J. (2006). Robust responses of the hydrological cycle to global warming. *Journal of Climate*, *19*(21), 5686 - 5699. doi: 10.1175/JCLI3990.1

Highwood, E. J., & Hoskins, B. J. (1998). The tropical tropopause. *Quarterly Journal of the Royal Meteorological Society*, *124*(549), 1579-1604. doi: https://doi.org/10.1002/qj.49712454911

Hu, S., & Vallis, G. K. (2019). Meridional structure and future changes of tropopause height and temperature. *Quarterly Journal of the Royal Meteorological Society*, *145*(723), 2698-2717. doi: https://doi.org/10.1002/qj.3587

Ingram, W. (2010). A very simple model for the water vapour feedback on climate change. *Quarterly Journal of the Royal Meteorological Society*, *136*(646), 30-40.

Jeevanjee, N. (2023, 09). Climate sensitivity from radiative-convective equilibrium: A chalkboard approacha). *American Journal of Physics*, *91*(9), 731-745. doi: 10.1119/5.0135727

Jeevanjee, N., & Fueglistaler, S. (2020a). On the cooling-to-space approximation. *Journal of the Atmospheric Sciences*, *77*(2), 465 - 478. doi: https://doi.org/10.1175/JAS-D-18-0352.1

Jeevanjee, N., & Fueglistaler, S. (2020b). Simple spectral models for atmospheric radiative cooling. *Journal of the Atmospheric Sciences*, *77*(2), 479 - 497. doi: https://doi.org/10.1175/JAS-D-18-0347.1

Jeevanjee, N., Koll, D. D. B., & Lutsko, N. (2021). "simpson's law" and the spectral cancellation of climate feedbacks. *Geophysical Research Letters*, *48*(14), e2021GL093699. doi: https://doi.org/10.1029/2021GL093699

Jeevanjee, N., & Romps, D. M. (2018). Mean precipitation change from a deepening troposphere. *Proceedings of the National Academy of Sciences*, *115*(45), 11465-11470. doi: 10.1073/pnas.1720683115

Jeevanjee, N., Seeley, J. T., Paynter, D., & Fueglistaler, S. (2021). An analytical model for spatially varying clear-sky co2 forcing. *Journal of Climate*, *34*(23), 9463 - 9480. doi: https://doi.org/10.1175/JCLI-D-19-0756.1

Kang, S. M., Frierson, D. M. W., & Held, I. M. (2009). The tropical response to extratropical thermal forcing in an idealized gcm: The importance of radiative feedbacks and convective parameterization. *Journal of the Atmospheric Sciences*, *66*(9), 2812 - 2827. doi: 10.1175/2009JAS2924.1

Koll, D. B., & Cronin, T. W. (2018). Earth's outgoing longwave radiation linear due to h2o greenhouse effect. *Proceedings of the National Academy of Sciences*, *115*(41), 10293-10298. doi: 10.1073/pnas.1809868115

Koll, D. D. B., Jeevanjee, N., & Lutsko, N. J. (2023). An analytic model for the clear-sky longwave feedback. *Journal of the Atmospheric Sciences*. doi: https://doi.org/10.1175/JAS-D-22-0178.1

Lin, P., Paynter, D., Ming, Y., & Ramaswamy, V. (2017). Changes of the tropical tropopause layer under global warming. *Journal of Climate*, *30*(4), 1245 -

1258. Retrieved from https://journals.ametsoc.org/view/journals/clim/30/4/jcli-d-16-0457.1.xml doi: 10.1175/JCLI-D-16-0457.1

Manabe, S., & Strickler, R. F. (1964). Thermal equilibrium of the atmosphere with a convective adjustment. *Journal of Atmospheric Sciences*, *21*(4), 361 - 385. doi: https://doi.org/10.1175/1520-0469(1964)021⟨0361:TEOTAW⟩2.0.CO;2

Match, A., & Gerber, E. P. (2022). Tropospheric expansion under global warming reduces tropical lower stratospheric ozone. *Geophysical Research Letters*, *49*(19), e2022GL099463. doi: https://doi.org/10.1029/2022GL099463

Meraner, K., Mauritsen, T., & Voigt, A. (2013). Robust increase in equilibrium climate sensitivity under global warming. *Geophysical Research Letters*, *40*(22), 5944-5948. doi: https://doi.org/10.1002/2013GL058118

Mlawer, E. J., Taubman, S. J., Brown, P. D., Iacono, M. J., & Clough, S. A. (1997). Radiative transfer for inhomogeneous atmospheres: Rrtm, a validated correlated-k model for the longwave. *Journal of Geophysical Research: Atmospheres*, *102*(D14), 16663-16682. doi: https://doi.org/10.1029/97JD00237

Mote, P. W., Rosenlof, K. H., McIntyre, M. E., Carr, E. S., Gille, J. C., Holton, J. R., ... Waters, J. W. (1996). An atmospheric tape recorder: The imprint of tropical tropopause temperatures on stratospheric water vapor. *Journal of Geophysical Research: Atmospheres*, *101*(D2), 3989-4006. doi: https://doi.org/10.1029/95JD03422

Nakajima, S., Hayashi, Y.-Y., & Abe, Y. (1992). A study on the "runaway greenhouse effect" with a one-dimensional radiative–convective equilibrium model. *Journal of Atmospheric Sciences*, *49*(23), 2256 - 2266. doi: https://doi.org/10.1175/1520-0469(1992)049⟨2256:ASOTGE⟩2.0.CO;2

Neale, R. B., & Hoskins, B. J. (2000). A standard test for agcms including their physical parametrizations: I: the proposal. *Atmospheric Science Letters*, *1*(2), 101-107. doi: https://doi.org/10.1006/asle.2000.0022

O'Gorman, P. A., & Schneider, T. (2008). The Hydrological Cycle over a Wide Range of Climates Simulated with an Idealized GCM. *Journal of Climate*, *21*(15), 3815. doi: 10.1175/2007JCLI2065.1

O'Gorman, P. A. (2011). The effective static stability experienced by eddies in a moist atmosphere. *Journal of the Atmospheric Sciences*, *68*(1), 75 - 90. doi: 10.1175/2010JAS3537.1

Phillips, N. A. (1956). The general circulation of the atmosphere: A numerical experiment. *Quarterly Journal of the Royal Meteorological Society*, *82*(352), 123-164. doi: https://doi.org/10.1002/qj.49708235202

Pierrehumbert, R. T. (2010). *Principles of planetary climate*. Cambridge University Press. doi: 10.1017/CBO9780511780783

Randel, W. J., & Jensen, E. J. (2013). Physical processes in the tropical tropopause layer and their roles in a changing climate. *Nature Geoscience*, *6*(3), 169–176. Retrieved from https://doi.org/10.1038/ngeo1733 doi: 10.1038/ngeo1733

Romps, D. M. (2016). Clausius–clapeyron scaling of cape from analytical solutions to rce. *Journal of the Atmospheric Sciences*, *73*(9), 3719 - 3737. doi: https://doi.org/10.1175/JAS-D-15-0327.1

Schneider, T. (2004). The tropopause and the thermal stratification in the extratropics of a dry atmosphere. *Journal of the Atmospheric Sciences*, *61*(12), 1317 - 1340. doi: https://doi.org/10.1175/1520-0469(2004)061⟨1317:TTATTS⟩2.0.CO;2

Schneider, T. (2008). Chapter 3 the thermal stratification of the extratropical troposphere. In *The global circulation of the atmosphere* (pp. 47–77). Princeton: Princeton University Press. doi: doi:10.1515/9780691236919-005

Schneider, T., O'Gorman, P. A., & Levine, X. J. (2010). Water vapor and the dynamics of climate changes. *Reviews of Geophysics*, *48*(3). doi: https://doi.org/10.1029/2009RG000302

Schneider, T., & O'Gorman, P. A. (2008). Moist convection and the thermal stratification of the extratropical troposphere. *Journal of the Atmospheric Sciences*, *65*(11), 3571 - 3583. doi: 10.1175/2008JAS2652.1

Seeley, J. T., Jeevanjee, N., & Romps, D. M. (2019). Fat or fitt: Are anvil clouds or the tropopause temperature invariant? *Geophysical Research Letters*, *46*(3), 1842-1850. doi: https://doi.org/10.1029/2018GL080096

Seidel, S. D., & Yang, D. (2022). Temperatures of anvil clouds and radiative tropopause in a wide array of cloud-resolving simulations. *Journal of Climate*, *35*(24), 8065 - 8078. doi: https://doi.org/10.1175/JCLI-D-21-0962.1

Simpson, G. C. (1928). Further studies in terrestrial radiation. *Monthly Weather Review*, *56*(8), 322 - 323. doi: https://doi.org/10.1175/1520-0493(1928)56⟨322:FSITR⟩2.0.CO;2

Spaulding-Astudillo, F. E., & Mitchell, J. L. (2023). Effects of varying saturation vapor pressure on climate, clouds, and convection. *Journal of the Atmospheric Sciences*, *80*(5), 1247 - 1266. doi: https://doi.org/10.1175/JAS-D-22-0063.1

Stevens, B., & Bony, S. (2013, 06). Water in the atmosphere. *Physics Today*, *66*(6), 29-34. doi: 10.1063/PT.3.2009

Stevens, B., & Kluft, L. (2023). A colorful look at climate sensitivity. *EGUsphere*, *2023*, 1–24. doi: 10.5194/egusphere-2022-1460

Stone, P. H., & Carlson, J. H. (1979). Atmospheric lapse rate regimes and their parameterization. *Journal of Atmospheric Sciences*, *36*(3), 415 - 423. doi: https://doi.org/10.1175/1520-0469(1979)036⟨0415:ALRRAT⟩2.0.CO;2

Tan, Z., Lachmy, O., & Shaw, T. A. (2019). The sensitivity of the jet stream response to climate change to radiative assumptions. *Journal of Advances in Modeling Earth Systems*, *11*(4), 934-956. doi: https://doi.org/10.1029/2018MS001492

Thompson, D. W. J., Bony, S., & Li, Y. (2017). Thermodynamic constraint on the depth of the global tropospheric circulation. *Proceedings of the National Academy of Sciences*, *114*(31), 8181-8186. doi: 10.1073/pnas.1620493114

Thompson, D. W. J., Ceppi, P., & Li, Y. (2019). A robust constraint on the temperature and height of the extratropical tropopause. *Journal of Climate*, *32*(2), 273 - 287. doi: https://doi.org/10.1175/JCLI-D-18-0339.1

Thuburn, J., & Craig, G. C. (2000). Stratospheric influence on tropopause height: The radiative constraint. *Journal of the Atmospheric Sciences*, *57*(1), 17 - 28. doi: https://doi.org/10.1175/1520-0469(2000)057⟨0017:SIOTHT⟩2.0.CO;2

Thuburn, J., & Craig, G. C. (2002). On the temperature structure of the tropical substratosphere. *Journal of Geophysical Research: Atmospheres*, *107*(D2), ACL 10-1-ACL 10-10. doi: https://doi.org/10.1029/2001JD000448

Vallis, G. K. (2017). *Atmospheric and oceanic fluid dynamics: Fundamentals and large-scale circulation* (2nd ed.). Cambridge University Press. doi: 10.1017/9781107588417

Vallis, G. K. (2020). The trouble with water: Condensation, circulation and climate. *The European Physical Journal Plus*, *135*(6), 478. doi: 10.1140/epjp/s13360-020-00493-7

Vallis, G. K., Colyer, G., Geen, R., Gerber, E., Jucker, M., Maher, P., ... Thomson, S. I. (2018). Isca, v1.0: a framework for the global modelling of the atmospheres of earth and other planets at varying levels of complexity. *Geoscientific Model Development*, *11*(3), 843–859. doi: 10.5194/gmd-11-843-2018

Vallis, G. K., Zurita-Gotor, P., Cairns, C., & Kidston, J. (2015). Response of the large-scale structure of the atmosphere to global warming. *Quarterly Journal of the Royal Meteorological Society*, *141*(690), 1479-1501. doi: https://doi.org/10.1002/qj.2456

Voigt, A., & Shaw, T. A. (2015). Circulation response to warming shaped by radiative changes of clouds and water vapour. *Nature Geoscience*, *8*(2), 102–106. doi: 10.1038/ngeo2345

Zurita-Gotor, P., & Vallis, G. K. (2011). Dynamics of midlatitude tropopause height in an idealized model. *Journal of the Atmospheric Sciences*, *68*(4), 823 - 838. doi: https://doi.org/10.1175/2010JAS3631.1